A Miniature Neural Recording Device to Investigate Sleep and Temperature Regulation in Mice

Bryan Hsieh*†‡, Edward C. Harding‡, William Wisden‡, Nicholas P. Franks‡, Timothy G. Constandinou*†
*Department of Electrical and Electronic Engineering, Imperial College London, SW7 2BT, UK
†Centre for Bio-Inspired Technology, Institute of Biomedical Eng., Imperial College London, SW7 2AZ, UK
‡Department of Life Sciences, Imperial College London, London, United Kingdom
Email:{bryan.hsieh12, e.harding11, w.wisden, n.franks, t.constandinou}@imperial.ac.uk

***Abstract*—Sleep is an important and ubiquitous process that, despite decades of research, a large part of its underlying biological circuity still remain elusive. To conduct research in this field, many devices capable of recording neural signals such as LFP and EEG have been developed. However, most of these devices are unsuitable for sleep studies in mice, the most commonly used animals, due to their size and weight. Thus, this paper presents a novel 4 channel, compact (2.1cm by 1.7cm) and lightweight (3.6g) neural-logging device that can record for 3 days on just two 0.6g zinc air 312 batteries. Instead of the typical solution of using multiple platforms, the presented device integrates high resolution EEG, EMG and temperature recordings into one platform. The onboard BLE module allows the device to be controlled wirelessly as well as stream data in real time, enabling researchers to check the progress of the recording with minimal animal disturbance. The device demonstrates its ability to accurately record EEG and temperature data through the long 24 hour in-vivo recordings conducted. The obtained EEG data could be easily sleep scored and the temperatures values were all within expected physiological range.**

Index Terms*—Neural recording, Wireless device, Micro device, Sleep analysis

I. Introduction

Sleep is an ubiquitous biological process that is found in most mammals and plays a major role in memory consolidation, cognitive performance and alertness. Some studies have also shown that sleep has association with certain neurological diseases as it was reported that REM sleep behavior disorder (RBD) could be used as an early marker for Parkinson's and dementia [1], [2].

Sleep studies have traditionally been carried out on small rodents, in particular transgenic mice, which places a limit on the size and weight of the device used for neural recording. There are many physiological factors that can affect sleep therefore with growing popularity in this field, there has been a steady increase in the demand for more and more sophisticated devices that can measure both neurological signals (EEG, ECoG) and also other physiological signals such as temperature, whilst still conforming to the limitations placed. Despite the rapid development of neural logging devices most of them that are currently on the market are still too big and heavy for sleep studies that involve mice as shown by Table. II. The device should weigh $<$ 10% of the body weight of the animal (typical adult mice weigh 20-30g) , untethered and be as small as possible to keep disturbance to the animal to a minimum, whilst having a minimum battery life of two days.

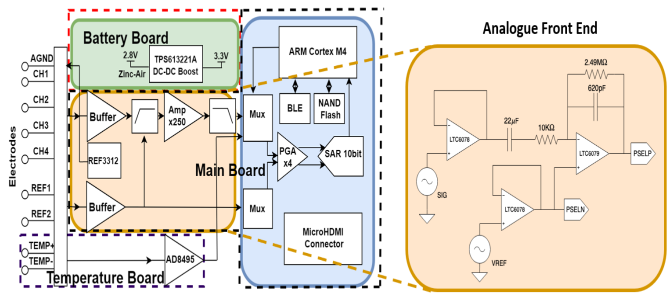

Fig. 1. Device Architecture

With the above in mind, this paper presents a 4 channel, compact (2.1cm by 1.7cm) and light weight (3.6g with batteries) neural-logging device that can measure and record EEG/EMG and temperature signals for more than 3 days. The device has a sample rate of 200 Hz and a low input referred noise (1-100 Hz) of $0.495\,\mu V_{rms}$. The data is stored on the onboard 4Gb NAND Flash memory that can be downloaded in 450s. The integrated BLE module allows the device to be controlled wirelessly as well as steam data in real time.

II. Device Workflow

To start a recording, first insert two zinc air 312 batteries into the device and check that it is advertising with the Android app. Then insert the device into a mouse that has a head stage connector implanted. Connect to the device by using the app and recording can be started by pressing the "Start Sampling" button. At the end of the experiment, connect to the device again and recording can be stopped by pressing the "Stop Sampling" button. The logger can then be removed and data can be downloaded by connecting the device to the downloader. During the experiment, the user can connect to and stream data from the device in real time at any given moment to check device operation.

III. Device Implementation

The device architecture is shown in Figure. 1. It consists of two boards, the main board and the battery board. The main

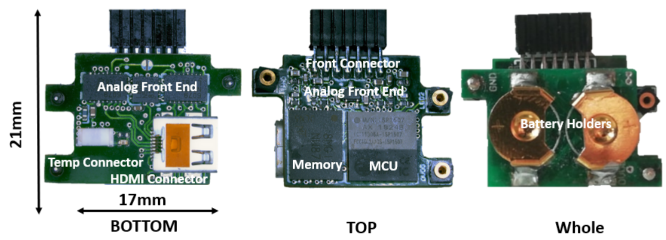

Fig. 2. Top, bottom and assembled views of the device

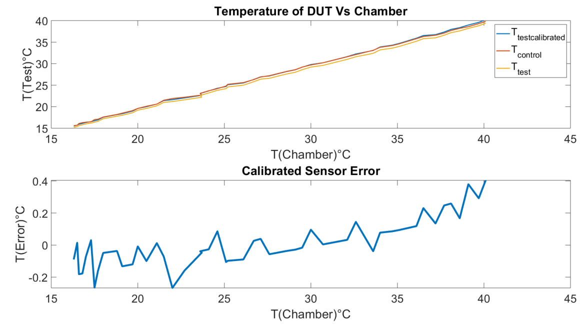

Fig. 3. Device temperature measurement error against a pre-calibrated thermocouple reader(Omega HH1384)

board has the analogue front end circuity for signal amplification, filtering and a digital back-end for data sampling, storage and BLE communication. The battery board hosts the power management circuity. The two boards are connected by the three one pin headers at the edges.

A. Analogue Front End

The analogue front end is a simple 2nd order band pass filter (2-120 Hz) with a pass-band gain of 48 dB and uses low noise ($18nV/\sqrt{Hz}$) and low power ($50\mu A$ per channel) LTC6079 opamps. The reference and signal inputs are buffered as they are connected to nodes that require a low source impedance. REF3312 from Texas Instruments is used to generate the 1.2V bias for the brain. The outputs of the analogue front end are connected directly to the PGA(G = 4) in the differential SAR ADC module.

B. Digital Back End

The digital back-end is powered by the NRF52832 SoC from Nordic, which contains an ARM Cortex M4 CPU and a Bluetooth 5 module. The MCU samples and stores the data from the differential ADC onto the NAND flash memory, which is organised into pages and blocks. Each page has 2048 bytes of main memory and 128 bytes of spare memory. The main memory holds exactly 256 samples of data and the spare memory holds the temperature data and also the bad block marker. This means with a sampling rate of 200 Hz, data is written to the NAND flash only once every 1.28 seconds, thus saving a significant amount of power. A custom BLE service and Android App are used to start/stop the device and stream the selected channel's data in real time through BLE notification events.

C. Temperature Sensing Board

A micro four pin JST header (SM04B-XSRS-ETB) on the main device is used to connect the device to a daughter temperature sensing board. The temperature sensing board contains an AD8945 K type thermocouple amplifier that has onboard cold junction compensation and an analogue output of $5mV/°C$.

D. Battery Board

The battery board contains the TPS613221A DC-DC boost converter to boost the 2.8V voltage from the zinc air 312 batteries to 3.3V. The device is shown in Figure. 2.

IV. Device Characterisation

A. Temperature Measurement Accuracy

AD8495 is a K type thermocouple amplifier, however a T type thermocouple is used in this device as the thermocouple will be inserted either into the body or cortical tissue and T type thermocouples are more suitable for humid environments. A humidity and temperature chamber (ESPEC SH-221) and a thermocouple reader (Omega HH1384) were used to calibrate the device. The readings from the reader were compared with the readings from AD8495 over the temperature range of $15°C - 40°C$ set by the chamber and the conversion factor from voltage to temperature was adjusted accordingly. After calibration, the device is accurate to $0.3°C$ as shown by Figure. 3.

B. BLE Performance

The device's bluetooth range at 4dBm radio power is around 4 meters when unobstructed. This range allows the device to be controlled from outside the animal holding room. However due to the limited bandwidth of BLE, the device can only stream one data channel at any given time.

C. Data Download

Data is downloaded off the device through a USB to SPI bridge (FTDI F232H). Due to the NAND flash used not supporting continuous read operation, data can only be downloaded one page at a time. This limits the total download time to 450s when SPI clock is set 16 MHz. However the 4Gb memory is enough for nearly 4 days of recording, therefore for a typical experiment that only lasts a day the download time is less than 2 minutes. The total number of pages to download along with the start date/time of the experiment are stored on two spaced out blocks (10 and 100) of the NAND flash to avoid memory corruption from bad blocks. These information are automatically read by the client software during data download.

D. Power Consumption

To ensure the device is as low power as possible, the MCU is configured to only wake on interrupt events and the ADC module is switched off in between sampling events. This results in the device only drawing a total of 1mA during sampling. However this current consumption increases to 1.1mA when a central BLE device is connected to the device and further to 2.2mA when the device starts sending notification packets (data streaming). The power consumption can be reduced by increasing the BLE advertising and connection intervals, however this also results in the increase in the time taken for a central device to connect to the device and a decrease in the data transfer speed. The break down of current consumption is shown in Figure. 4.

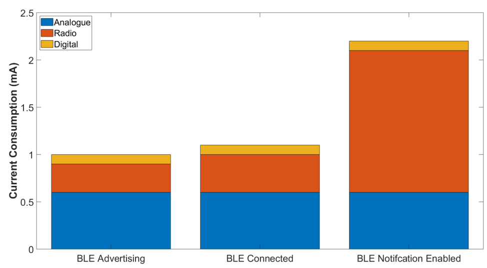

Fig. 4. Breakdown of power consumption

E. Battery Life

The device is powered by zinc air batteries as they have the highest energy density out of all coin cell batteries. However they have a very low maximum discharge rate. Hence it is important to ensure the batteries can power the device and are stable for the entire duration of the experiment. The battery life was measured using a DC power analyzer (N6705C) over a period of three days at a sampling interval of 100ms. Figure. 5 shows the effects of sudden increase in power consumption from NAND write/erase and BLE events on the battery voltage. It also shows that it took a few hours for the battery voltage to stabilise but once it did, both the battery and regulator voltages stayed constant throughout the remainder of the experiment.

V. Experimental Results

A. Headstage Implantation

A surgical setup had already been devised for the logger currently used in the lab, therefore to be compatible with the current surgical setup, the device also uses the same seven pin (4 channels, 2 references and 1 GND) 1.27mm pitch

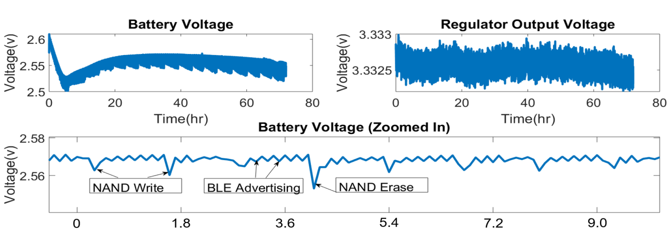

Fig. 5. Battery life of the device measured using DC power analyzer N6705C

connector to interface with the animal. To prepare the animal for headstage docking, three m1 metal screws, which are used as the electrodes, are inserted into locations REF (1.5mm, 1.5mm), EEG1 (-1.5mm, -1.5mm) from bregma and EEG2 (0mm , -5mm) from lambda as shown in Figure. 6A. The two EMG wires are slid under the neck muscles. Wires are then attached to the screws and also to the headstage connector and everything is sealed off with a mixture of dental cement and glue as shown in Figure. 6B.

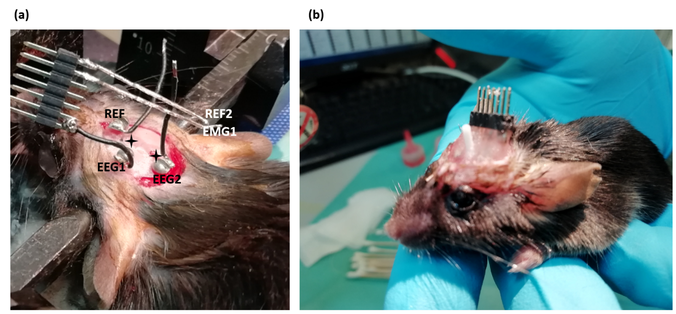

Fig. 6. Headstage surgery. The locations of the electrodes are shown relative to bregm (top star) and lambda (bottom star)

B. Long EEG Recording

A long 10 hour recording was conducted on a black strain mouse in its home cage. The obtained data were then sleep scored by using the OSD7 v7.2 script in Spike2 (data processing software). Sleep stage scoring is an important process whereby the data is split into epochs of 5-30s and each epoch is labelled a sleep stage (Wake, NREM and REM) according to its delta, theta and EMG powers. Wake is defined as having high EMG but low delta power, NREM is defined as having low EMG but high delta powers and REM is defined as having a low EMG but high theta/delta ratio. Therefore it is important that there are clear distinctions between high and low levels in the EMG, theta and delta powers. This is evidently shown in Figure. 7A. The power spectrum and wavelet transform [3] in Figure. 7B show the shift in the dominating frequency from theta to delta and then the increase in delta power, when the animal changes state from wake to NREM and then to REM. The observed results are in agreement with many publications [4], [5].

C. Long Temperature Recording

To record cortical temperature, the temperature daughter board was glued onto the headstage connector, then a T type thermocouple (5TC-TT-TI-40-1M) was inserted into the hippocampus of the animal with an insertion depth of 1mm, shown in Figure. 8B. The thermocouple used has a small diameter of 0.08mm which minimizes tissue damage. Figure. 8A shows the recorded cortical temperature over 24 hours. The animal was under isoflurane (an anaesthetic) and then moved into a heat box ($36°C$) before being put back to its home cage, hence the initial lower temperature. The baseline temperature is lower than expected at $34°C$ and oscillates during sleep

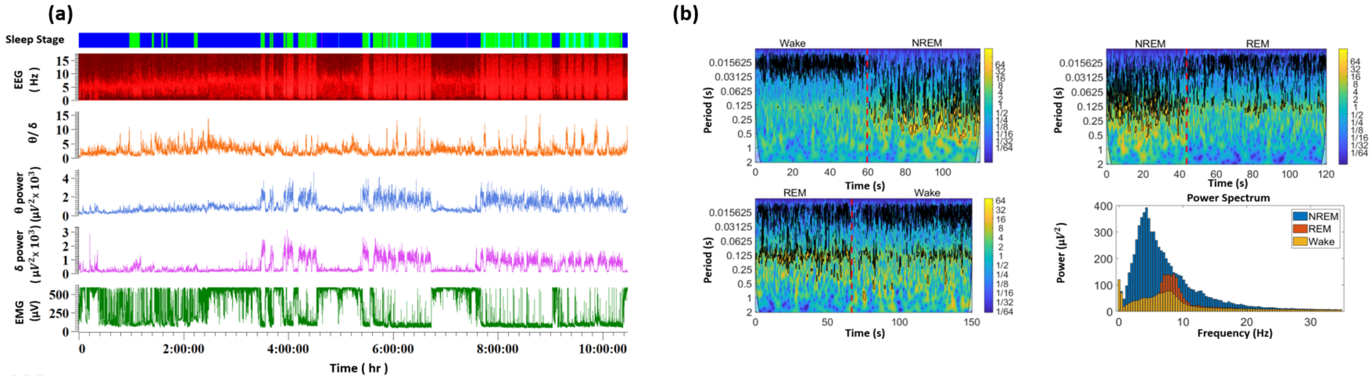

Fig. 7. (a)EEG recording taken from Spike2, the scored sleep epochs are shown in the stage channel. (Blue = Wake, Green = NREM, Light Blue = REM) ,(b)power spectrum and wavelet transform, black contour indicates the 5% significance level

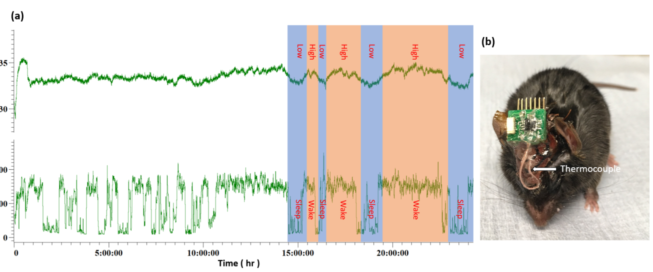

Fig. 8. 24 hour temperature and EMG recording

TABLE I

Table of current device specifications

Power Supply	2.7 V	Current Consumption	1 mA
Number of Channels	4	Temperature Accuracy	$0.3\,^{\circ}C$
Filter 3dB Bandwidth	2-120 Hz	Temperature Sampling Rate	0.5 Hz
Input Dynamic Range	52 dB	On Board Memory	4 Gb
Input Referred Noise of AFE	$0.495\mu V$ uVrms	Download Time	450 s
THD of AFE	-64.3 dBc	Data Streaming	BLE
ADC Resolution	9 bit (ENOB)	Size	2.1 cm x 1.7 cm x 1 cm
ADC Sampling Rate	200 Hz	Weight	3.6 g
Oversample	4x	Battery Life	$> 72\,hr$

TABLE II

Current State of the Art

	JAGA Penny	Multichannel Systems W21000-HS8	Vyssotski Neurologger 2A	Proposed Device
Number of Channels	16	8	4	4
Bandwidth(Hz)	0.1-300	1-400	n/a	2-100
Bit Resolution	16	16	10	9
Sampling Rate (Sps/s)	1k	1k	0.6-19.2k	200
Data Acquisition	Wireless	Wireless	1GB onboard Memory	500MB / Wireless
Noise(rms)	$2.7\mu V$	$1.9\mu V$	n/a	$0.495\mu V$
Device Weight (g)	1.9	3	2.2	2.4
Battery Weight (g)	1.2-12	1.2-12	1.2	1.2
Battery Life (h)	1.5-24	2	48+	72+
Device Size	24 x 15.4 x 3 mm	15.5 x 15.5 x 5.2 mm	22 x 15 x 5 mm	21 x 17 x 10 mm

and wake stages in the lights off period only. More trials are needed to see if this behviour is significant. Nevertheless all temperature values were within the accepted physiological range.

VI. Conclusion

A compact, low power (1mA) 4 channel EEG/EMG and temperature logging device is presented in this paper. Its small size (2.1cm by 1.7cm) and light weight (3.6g with batteries) make it ideal to be used in sleep studies involving small rodents such as mice. The inclusion of a temperature sensor for cortical temperature recording and the integration of BLE radio to allow user to control and stream data in real time have made the device able to compete with top devices on the market as shown by table II. The device has demonstrated that it can accurately record EEG/EMG signals that can be used in sleep stage scoring. Powered by two zinc air 312 batteries, the device can record for over three days which is adequate for most sleep experimental work and longer than any other devices.

References

[1] A. Iranzo, J. L. Molinuevo, J. Santamaría, M. Serradell, M. J. Martí, F. Valldeoriola, and E. Tolosa, "Rapid-eye-movement sleep behaviour disorder as an early marker for a neurodegenerative disorder: a descriptive study," *The Lancet Neurology*, vol. 5, no. 7, pp. 572–577, 2006.

[2] R. B. Postuma, J. F. Gagnon, M. Vendette, M. L. Fantini, J. Massicotte-Marquez, and J. Montplaisir, "Quantifying the risk of neurodegenerative disease in idiopathic REM sleep behavior disorder." *Neurology*, vol. 72, no. 15, pp. 1296–300, 4 2009. [Online]. Available: http://www.ncbi.nlm.nih.gov/pubmed/19109537 http://www.pubmedcentral.nih.gov/articlerender.fcgi?artid=PMC2828948

[3] A. Grinsted, J. C. Moore, and S. Jevrejeva, "Nonlinear Processes in Geophysics Application of the cross wavelet transform and wavelet coherence to geophysical time series," Tech. Rep., 2004. [Online]. Available: http://www.pol.ac.uk/home/research/waveletcoherence/

[4] M. Panagiotou, K. Papagiannopoulos, J. H. Rohling, J. H. Meijer, and T. Deboer, "How old is your brain? Slow-wave activity in non-rapid-eye-movement sleep as a marker of brain rejuvenation after long-term exercise in mice," *Frontiers in Aging Neuroscience*, vol. 10, no. AUG, 8 2018.

[5] J. M. Petit, S. Burlet-Godinot, P. J. Magistretti, and I. Allaman, "Glycogen metabolism and the homeostatic regulation of sleep," *Metabolic Brain Disease*, vol. 30, no. 1, pp. 263–279, 2014.